



ELSEVIER

Fluid Phase Equilibria, 100 (1994) 1–34

---

---

FLUID PHASE  
EQUILIBRIA

---

---

## The Lennard-Jones fluid: An accurate analytic and theoretically-based equation of state

Jiří Kolafa and Ivo Nezbeda

*E. Hála Laboratory of Thermodynamics, Institute of Chemical Process Fundamentals,  
Academy of Sciences, 165 02 Prague 6-Suchbát, Czech Republic*

(Received April 14, 1994; accepted in final form July 12, 1994)

**Keywords:** theory, equation of state, computer simulation, perturbed hard spheres, perturbed virial expansion, molecular-thermodynamic reference, Lennard-Jones fluid

### ABSTRACT

A new analytic equation of state for the Lennard-Jones fluid is proposed. The equation is based on a perturbed virial expansion with a theoretically defined temperature-dependent reference hard sphere term. The expansion is written for the Helmholtz free energy which guarantees the thermodynamic consistency of the pressure and internal energy. The equation covers much wider range of temperatures (up to seven times the critical temperature) than existing equations and is significantly more accurate and has less parameters than the best equation available to date, the modified Benedict-Webb-Rubin equation due to Johnson, Zollweg, and Gubbins (1993, *Mol. Phys.* 78: 591–618). As a side-product, highly accurate explicit analytic correlations of the hard sphere diameters, as given by both the hybrid Barker-Henderson and Weeks-Chandler-Andersen theories, have been obtained.

Computer simulation data to be regressed by the equation have been compiled from several sources and critically assessed. It has been shown that many literature data for state points with a large compressibility are subject to large systematic finite-size errors. Additional simulations on a series of systems of different sizes have been therefore performed to facilitate the extrapolation to the thermodynamic limit in the region close to the critical point.

### INTRODUCTION

Despite the great progress of molecular theories of liquids achieved over the last three decades, the impact of all the achievements on engineering practice has been practically zero. One reason is evident: the dependence of results on the chosen potential model and ignorance of the precise form of actual intermolecular forces. Another reason why engineers are reluctant to adopt theoretical results, is their usual complexity and, what is even more important, insufficient accuracy.

The former deficiency is relevant when we deal with real fluids and statistical mechanics applied to them may thus provide only guidance towards useful analytic results (for instance, functional formulas which may be used to correlate experimental data) but not final answers. However, this deficiency has nothing to do with studies of model fluids defined unambiguously by a potential model. It is therefore more than startling to watch theorists betraying their own results and recommendations in situations calling for their implementations. To be more specific, let us consider the Lennard-Jones 12-6 (LJ) fluid which may serve as a remarkable example. When facing the practical problem to parameterize the existing computer simulation data on pressure, even top theorists, instead of using the fundamental result of molecular theory of liquids and writing the equation of state (EOS) in a form of a perturbation expansion with the reference term corresponding to a system with short-ranged repulsive forces, have always resorted either to a modified Benedict-Webb-Rubin (MBWR) equation with 33 parameters or to other purely empirical equations. References to all these attempts may be found in a recent paper by Johnson *et al.* (1993). In the light of this fact everybody must question the usefulness of the molecular approach for engineering applications at all and the truthfulness of all the boastful phrases introducing theoretical papers.

The LJ potential is undoubtedly the most popular and prominent model among all the realistic potential models used in theories of liquids. It approximates reasonably well, at normal conditions, both the repulsive and attractive parts of the actual interactions between molecules of simple fluids and it is therefore used also as an atom-atom (or, more generally, site-site) potential in site-site potential models of polyatomic molecules (Maitland *et al.*, 1987). Since we have always believed in usefulness of statistical mechanical theories of liquids, we have embarked on a project whose ultimate goal has been to show that the thermodynamic properties of the LJ fluid can be described analytically by a perturbed hard-sphere EOS with accuracy better or at least comparable to that of purely empirical equations.

In previous papers (Nezbeda and Aim, 1984, 1987, and 1989, and Nezbeda, 1993) we reported partial results along the path aiming at the above ultimate goal and proved its attainability. Our approach is based on the concept of a molecular-thermodynamic reference equation of state (Nezbeda, 1993, hereafter referred to as paper I) in which the final complete equation has the form of a perturbed hard-sphere EOS with one (or more) theoretically-based term(s) and an empirical correction term. The present paper accomplishes the project by presenting such an accurate analytic EOS for the LJ fluid.

In paper I two different sets of molecular-thermodynamic references (MTR) were considered: one corresponding to the well-known first-order perturbation expansions and the other called perturbed virial expansion. Having been guided by a reasonable performance, in general, of the former theories, we tended to prefer them also for the choice of the MTR. The idea behind this choice was that the residual properties, *i.e.* the difference between the simulated and MTR results, were small and should be thus amenable to a simple empirical

parameterization, not necessarily extremely accurate. We followed therefore this route but were gradually encountering difficulties. Although the residual pressure was small, its temperature and density dependence turned out to be so complicated that we were not able to reach, with a reasonable number of adjustable parameters, an accuracy comparable to that of the best empirical EOS available to date, the MBWR-type equation due to Johnson *et al.* (1993), referred to henceforth as the JZG equation.

It turns out that the failure of the first-order perturbation expansions to serve as a good and useful MTR (over a wide range of thermodynamic conditions) has its origin in their incorrect low density limit. Once this deficiency is removed (by introducing a correction term), the overall accuracy of these theories is lost and, effectively, they become identical to the perturbed virial expansion. We have therefore based our new equation on the perturbed virial expansion.

To derive a semi-theoretical equation with a number of adjustable parameters, a large set of reliable experimental data must be available. For this purpose we have first reviewed and critically assessed the existing data and for the regions where no sufficiently accurate data have been available we performed our own simulations. A special attention has been paid to estimation of errors of all the data.

After summarizing all the theoretical prerequisites in the next Section, we undertake in the subsequent Section a detailed analysis of the computer simulation data, especially with respect to their estimated errors, and present a set of new simulation data for the states with a large compressibility. In the last Section we then present first a new and highly accurate parameterization of the temperature dependence of the reference hard spheres as it is defined by a modified Barker-Henderson perturbation theory (Smith, 1973). Our new analytic EOS is then presented and compared with the MBWR, JZG and other equations. The new equation is thermodynamically self-consistent which means that it yields results of a comparable accuracy for both the pressure and internal energy. Its accuracy for pressure is the same or slightly better than that of the JZG equation but its performance for the internal energy is much better. In the course of this study we have also obtained a very accurate explicit representation of the temperature and density dependence of the reference hard spheres as it is defined by the theory of Weeks, Chandler and Andersen (1971). This result has not been used, in the end, for developing the new EOS but with respect to its importance and general interest we present this result in *Appendix B*.

## THEORETICAL PREREQUISITES

The LJ fluid is defined by the pair potential

$$u(r) = 4\epsilon[(\sigma/r)^{12} - (\sigma/r)^6] \quad (1)$$

where  $\epsilon$  measures the strength of the interaction and  $\sigma$  is the collision diameter; throughout the paper henceforth we shall use only reduced variables, *i.e.* units

will be used such that  $\epsilon = \sigma = k_B = 1$  with  $k_B$  being the Boltzmann constant. The thermodynamic properties considered in the paper will mean (with the exception of pressure) the excess over the properties of the ideal gas; the term ‘residual’ will mean the excess over the properties of a reference system, *cf.* *Introduction*.

Theoretical methods applied to potentials of the LJ-type make extensive use of the present excellent knowledge of properties of the fluid of hard spheres (HS) defined by

$$\begin{aligned} u_{\text{HS}}(r) &= \infty & \text{for } r < d \\ &= 0 & \text{for } r > d \end{aligned} \quad (2)$$

where  $d$  is a sphere diameter. The properties of the HS fluid are defined by the packing fraction  $\eta$ ,

$$\eta = \frac{\pi}{6} \rho d^3 \quad (3)$$

by means of which an EOS used in this paper can be expressed as follows [see Boublík and Nezbeda, 1986, eqn. (4.46)]:

$$z_{\text{HS}} \equiv \frac{P_{\text{HS}}}{\rho T} = \frac{1 + \eta + \eta^2 - \frac{2}{3}\eta^3(1 + \eta)}{(1 - \eta)^3} \quad (4)$$

This equation, which slightly differs from the commonly used Carnahan-Starling equation, is by one order more accurate. The Helmholtz free energy associated with this EOS is

$$A_{\text{HS}} = T \left[ \frac{5}{3} \ln(1 - \eta) + \frac{\eta(34 - 33\eta + 4\eta^2)}{6(1 - \eta)^2} \right] \quad (5)$$

Another quantity which will be later required is the second virial coefficient defined, in general, by

$$B_2 = -\frac{1}{2} \int \{[1 - \exp[-u(r)/T]]\} d\mathbf{r} \quad (6)$$

where  $r = |\mathbf{r}|$ .

For the HS fluid we get from here

$$B_{2,\text{HS}} = \frac{2\pi}{3} d^3 \quad (7)$$

For the LJ fluid the above integral cannot be evaluated analytically in a closed form; its expression in the form of a fast converging series in powers of  $T^{-1/4}$  can be found in standard textbooks.

### Molecular-thermodynamic references

For applications of theoretical results to practical problems it has been suggested in paper I that a semi-theoretical expression for quantity  $X$  be searched for in the form

$$X = X_{\text{ref}} + \Delta X \quad (8)$$

where  $X_{\text{ref}}$  denotes  $X$  of a reference system,  $\Delta X$  is a correction term, given usually by an expansion in powers of a parameter(s), and  $X_{\text{ref}}$  and  $\Delta X$  are subject to the following constraints in order for (8) to be of any practical use: (i)  $\Delta X$  must be a small correction, which means that  $X_{\text{ref}}$  provides a reasonable zeroth-order approximation to  $X$ , (ii)  $X_{\text{ref}}$  must be available in a simple closed analytic form, and (iii)  $\Delta X$  must be a *simple* function of its variables. It turns out that the last condition is much more important than the first two.

To derive an EOS we take for  $X$  the Helmholtz free energy per particle,  $A$ , rather than pressure (or the compressibility factor) directly to guarantee the thermodynamic consistency; the required quantities are then obtained using the standard thermodynamic relationships:

$$P = \rho T + \rho^2 \frac{\partial A}{\partial \rho} \quad (9)$$

$$U = \frac{\partial(A/T)}{\partial(1/T)} \quad (10)$$

$$\mu = A + P/\rho - T \quad (11)$$

where  $U$  is the internal energy and  $\mu$  the chemical potential.

The two MTR's considered in paper I have been the first order perturbation expansion (HTA approximation),

$$A_{\text{ref}} \equiv A_{\text{HS+HTA}} = A_{\text{HS}} + A_{\text{HTA}} \quad (12)$$

and the perturbed virial expansion,

$$A_{\text{ref}} \equiv A_{\text{PVE}} = A_{\text{HS}} + \rho T \Delta B_2 \quad (13)$$

Both these references have their advantages and disadvantages. The former reference by itself provides a reasonable estimate of the properties of the LJ fluid throughout the entire  $\rho - T$  plane (Aim and Nezbeda, 1989) and its only drawback seems that it does not give the correct low density limit, *i.e.* the second virial coefficient. On the other hand, the latter reference reproduces  $B_{2,\text{LJ}}$  exactly but with increasing density the second term in (13) becomes unrealistically too large and, consequently, also the residual term  $\Delta A_{\text{PVE}} = A - A_{\text{PVE}}$ .

The mentioned drawbacks of the above references may be corrected by the residual terms  $\Delta A$  but this does not seem practical and would in fact contradict the spirit of the method. Both references must be therefore appropriately modified:

$$A'_{\text{HS+HTA}} = A_{\text{HS}} + A_{\text{HTA}} + (\rho T \Delta B_2 - A_{\text{HTA},0}) \exp(-\gamma \rho^2) \quad (14)$$

where  $A_{\text{HTA},0}$  denotes the limit  $\rho \rightarrow 0$  of  $A_{\text{HTA}}$ , and

$$A'_{\text{PVE}} = A_{\text{HS}} + \rho T \Delta B_2 \exp(-\gamma \rho^2) \quad (15)$$

The residual second virial coefficient  $\Delta B_2$  denotes the difference between the LJ and HS second virial coefficients,

$$\Delta B_2 = B_{2,\text{LJ}} - B_{2,\text{HS}} \quad (16)$$

The damping function  $\exp(-\gamma \rho^2)$  used in the above equations is only one of many possible choices; the same function appears *e.g.* also in the MBWR equation.

As soon as the above modifications are introduced, the difference between the two references smears out and, by including the  $A_{\text{HTA}}$  term into the residual term  $\Delta A$ , the HS+HTA theory becomes formally identical to the PVE. This is the reason why in the end we have abandoned the HS+HTA reference and in the following we will therefore use only the MTR given by eqn. (15).

### *Hard sphere diameters*

To implement eqn. (8) with the reference given by eqn. (15), a link of the HS fluid to the LJ fluid must be established. It means, recipes for the HS diameter in terms of the parameters and properties of the LJ fluid must be given.

We have always considered only the two well-known and rigorously defined choices, one called the hybrid Barker-Henderson (hBH) and given by (Smith, 1973; Nezbeda and Aim, 1984)

$$d_{\text{hBH}} = \int_0^{R_m} \{1 - \exp[-u_0(r)/T]\} dr \quad (17)$$

and the other due to Weeks-Chandler-Andersen given implicitly by the equation (Weeks *et al.* 1971)

$$\int_0^{R_m} y_{\text{HS}}(r; d_{\text{WCA}}) \{ \exp[-u_0(r)/T] - H(r > d_{\text{WCA}}) \} r^2 dr = 0 \quad (18)$$

where  $R_m$  is the location of the potential minimum,  $R_m = 2^{1/6}$  for the LJ fluid. The potential  $u_0$  in both these choices is the same and corresponds to the separation of the potential  $u$  at its minimum,

$$\begin{aligned} u_0(r) &= u(r) - u(R_m) & \text{for } r < R_m \\ &= 0 & \text{for } r > R_m \end{aligned} \quad (19)$$

Function  $y_{\text{HS}}(r; d)$  in (18) is the background correlation function of the fluid of hard spheres of diameter  $d$  and  $H$  is the function returning unity if the argument is true and zero otherwise.

From (17) it follows that  $d_{\text{hBH}}$  is only temperature-dependent, while the WCA reference HS diameter depends both on temperature and density. Although the latter dependence leads to a better performance of the theory, it is usually considered undesirable, mainly from the point of view of practical applications, because the resulting increase in complexity does not seem to be outweighed by the final results. Henceforth we will use only the hBH choice; the results for the WCA diameters are given in *Appendix B*.

## Functional approximations

To express a set of data by means of a mathematical formula is a typical engineering problem usually solved by fitting (many) parameters of polynomials or rational functions to the data. Two different approaches to approximate a given function by a formula are used in dependence whether the function to be approximated is known or not.

### Approximating exactly known functions

Several functions of temperature used in molecular theories (*e.g.* the density-independent diameter of the reference hard spheres and the second virial coefficient) are defined by integrals and are thus available with arbitrary precision. Our task is to express them by means of a simple closed formula, *e.g.* a polynomial. This is a standard task solved in the optimum way by the Chebyshev minimax approximation (see *e.g.* Ralston, 1965, Chap. 7.9). This means that the maximum error

$$\epsilon_{\max} = \max_x |f(x) - f_{\text{approx}}(x)| \quad (20)$$

for  $x$  in a given interval reaches the minimum from all functions  $f_{\text{approx}}(x)$  from a given set of functions. Before using this approximation we must realize that we do not need only an accurate approximation of these functions themselves, but also their derivatives with respect to the inverse temperature because these derivatives are (directly or indirectly) related to the internal energy. Since the derivative is normally subject to larger errors than the integrated function, we first approximate the derivatives by minimizing their maximum error  $\epsilon'_{\max}$  and then integrate them to get the final functional approximation. For the sake of simplicity we confine our approximations to polynomials only.

The required accuracy can be estimated by the influence of errors in the approximated functions on the errors in the quantities of interest, namely  $P$  and  $U$ , compared to the pseudoexperimental errors (see next Section). Thus, the accuracy of the reference HS diameter and its derivative over  $1/T$  should be of the order of  $1 \times 10^{-4}$ , the accuracy of the second virial coefficient and its derivative may be by one order lower.

### Correlation of inaccurately known data

If the function (generally of many variables) to be fitted is not available with arbitrary precision and we have only a set of data  $\{X_i\}_{i=1}^m$  instead, we use the least square method, *i.e.* we minimize the following sum of squares

$$\chi^2(\mathbf{p}) = \sum_{i=1}^m \frac{[X_{i,\text{calc}}(\mathbf{p}) - X_i]^2}{\delta X_i^2} \quad (21)$$

where  $\mathbf{p} = \{p_j\}_{j=1}^n$  is the set of parameters,  $X_{i,\text{calc}}$  is the value calculated from the correlator  $\hat{X}$ , and  $\delta X_i$  serves as inverse weight assigned to point  $i$ .

If the formula is able to describe the data then  $\delta X_i$  may be identified with the experimental error. The standard deviation defined by

$$D(\mathbf{p}) = \sqrt{\chi^2(\mathbf{p})/(m - n)} \quad (22)$$

then serves as a measure of the quality of the regression. As another measures of the quality we use the maximum deviation defined by

$$\delta_{\max} = \max_i \{|X_{i,\text{calc}} - X_i|/\delta X_i\} \quad (23)$$

and the partial standard deviation defined for a subset of data  $S$

$$D_S(\mathbf{p}) = \sqrt{\frac{1}{|S|} \sum_{i \in S} \frac{[X_{i,\text{calc}}(\mathbf{p}) - X_i]^2}{\delta X_i^2}} \quad (24)$$

Note that, unlike (22), the number of degrees of freedom  $n$  is not subtracted from  $|S|$  in (24).

If the formula is not capable to describe the data within the errors, then we must choose the weights assigned to the individual points, that is, we must decide how accurate fit is required in different regions.

## SIMULATION DATA AND THEIR ASSESSMENT

The LJ fluid has been intensively studied by means of computer simulations over the last three decades and a critical review of these data may be found in a paper by Aim and Nezbeda (1989). For the purpose of this work only top quality data can be used and we used therefore data coming only from four sources: Johnson *et al.* (1993), Lotfi *et al.* (1992), Kolafa *et al.* (1993), and data generated in the course of this study. All these data were critically reviewed with respect to possible systematic errors. Some of the data had to be removed and often unreliable error estimates had to be adjusted.

The extensive set of data by Johnson *et al.* (1993) was obtained mostly by MD with the cut-off and shifted potential and 864 atoms; some of them were also obtained using MC. The data cover the range of temperatures  $0.7 \leq T \leq 6$  and all possible densities including some metastable points.

The second set of data was taken from Tables 1 and 2 in Lotfi *et al.* (1992). The data were obtained in an NPT ensemble using as many as 1372 particles. The data include the chemical potential and cover the range around the vapor-liquid coexistence curve.

The third source of data was the paper by Kolafa *et al.* (1993) and the fourth one the new data summarized in Table 1.

As additional data for the use in the low density range we used the virial equation of state truncated after the fifth term. We evaluated accurately the second and third virial coefficients and the fourth and fifth ones were taken from Barker *et al.* (1966). The state points covered densities  $\rho \leq 0.1$  for supercritical temperatures and lower densities for the region  $1 < T < 1.3$ ; lower temperatures were not considered because for densities lower than the dew density the



TABLE 1

New MC and MD data for the LJ fluid. Infinity in the column for the number of particles  $N$  denotes the extrapolated value from  $N \in \{256, 512, 1024\}$

method	$N$	$T$	$\rho$	$P$	$\delta P$	$U$	$\delta U$
MD <sup>ab</sup>	864	0.81	0.8645	1.0954	0.0036	-6.10212	0.00053
MC <sup>c</sup>	$\infty$	1.2	0.5	0.02816	0.007	-3.4809	0.006
MD+MC	$\infty$	1.2	0.7	0.6710	0.006	-4.7593	0.0018
MC <sup>c</sup>	$\infty$	1.3	0.2	0.12113	0.00087	-1.5685	0.0038
MC <sup>c</sup>	$\infty$	1.3	0.4	0.1117	0.0045	-2.8293	0.008
MC <sup>c</sup>	$\infty$	1.3	0.5	0.15495	0.004	-3.4204	0.0025
MD+MC	$\infty$	1.3	0.6	0.35725	0.005	-4.0555	0.0026
MC <sup>c</sup>	$\infty$	1.4	0.2	0.15148	0.00081	-1.4912	0.003
MC <sup>c</sup>	$\infty$	1.4	0.4	0.19532	0.0045	-2.7597	0.0035
MC	$\infty$	1.45	0.3	0.1988	0.0012	-2.1179	0.0017
MD	1024	4.85	1.0	31.474	0.040	-2.2925	0.008
MD	512	10.0	1.0	54.032	0.030	1.4171	0.0060
MD	1024	10.0	1.2	99.178	0.060	5.4480	0.010

<sup>a</sup> Errors have been increased (see Section *Systematic errors*)

<sup>b</sup> Misprint in Kolafa *et al.* (1993) has been fixed

<sup>c</sup> These data replace the data by Johnson *et al.* (1993) in the final data set

second virial coefficient gives sufficiently accurate values and our EOS predicts the second virial coefficient correctly. From the virial expansion only pressure and chemical potential were calculated because the internal energy requires the derivative of the virial coefficients with respect to temperature and this was not directly available. The maximum errors were estimated from the fifth term; the ‘statistical errors’ serving as weights in the sum of squares (21) had to be increased because otherwise the resulting EOS would be too accurate in the low density region and would overweight the results in the interesting high-density region which would be then less accurate. (In an extreme case we would get the EOS fitting the virials and ignoring the dense liquid). We used errors of pressure (chemical potential) about 3–5 times smaller than the MD errors of pressure (internal energy) at the same points. Inclusion of the virial EOS can be thus viewed as an improvement of simulation data which are in the low density region less accurate. Inclusion of these data was important because it led to a significant change of the fitted parameters. On the other hand, the standard deviation  $D$  almost did not change which means that the errors were set consistently.

### Statistical errors

The averages of thermodynamic quantities are subject to experimental errors which are usually expressed as the standard deviation of the average. Then,

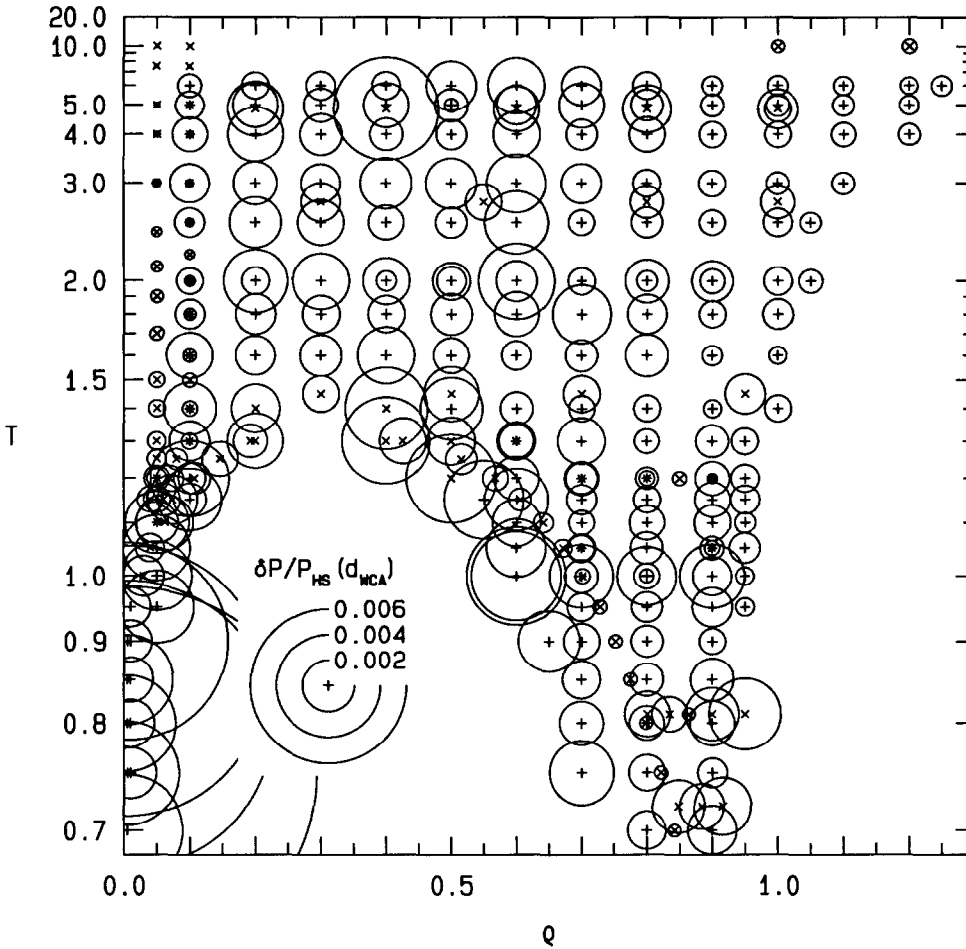
under the usual assumption of the Gaussian distribution of errors, we have a 68% chance that the correct expectation value lies within the error bars. This trivial statement assumes, however, that our estimates of the errors are accurate. We would like to stress here that the standard deviation of the average is a thermodynamic quantity which is, at the given experimental conditions (simulation time, frequency of measurements, etc.), defined as well as *e.g.* pressure. Quality and statistical properties of these error estimates come into effect if a large set of data is analyzed which is just the case of correlating the data by a formula.

The errors of the data by Johnson *et al.* (1993) were estimated by the block average method with only 10 subblocks and are thus inaccurate though (with possible exception of the critical region) not biased. Using the plausible assumption that the blocks are uncorrelated and the tables of the  $\chi^2$  distribution, one can estimate that in 1.3% of points the published error is less than 50% of the actual error, and thus the weight given to the corresponding square in the function to be minimized (21) is more than 4 times higher than it should be. Consequently, we had to re-adjust some of the errors using the assumption that the error is, for the simulation points obtained at similar conditions, a smooth function of temperature and density. In most cases we increased the error, in the worst case ten times, to obtain error comparable with the errors of the points in the neighbourhood. The second drawback of the data is that both the data and errors were rounded only to one decimal digit. To take into account these unnecessary additional errors we added 0.5 to the last significant digit of the errors. This means that in the worst case (about 25% of all cases), error of  $1 \times 10^n$  was changed to  $1.5 \times 10^n$ .

Lotfi *et al.* (1992) used an obscure method for the error estimation based on the course of the second half of the running average. According to our numerical tests (made for uncorrelated data and long runs) this method tends to overestimate the actual error by about 20%. The statistical properties of the method are not better than of the 10-subblock method. We thus applied the same adjusting procedure as above to get the uniformly behaving errors. Fortunately, the data were not debased by rounding. The data were obtained in an isobaric ensemble and thus we had to re-calculate the errors to an isochoric ensemble to make them consistent with other data. The equivalent error in  $P$  is simply  $\delta P = \delta \rho / (\beta_T \rho)$ , where  $\beta_T$  was also published. For the error in  $U$  we took the published values because it can be shown, by comparing different data, that the errors in  $U$  in the isochoric ensemble are smaller than in the isobaric ensemble. The error of  $\mu$  was obtained from the published error of  $\tilde{\mu} = \mu - \ln \rho$  by adding the relative error of  $\rho$ , which is the most pessimistic assumption.

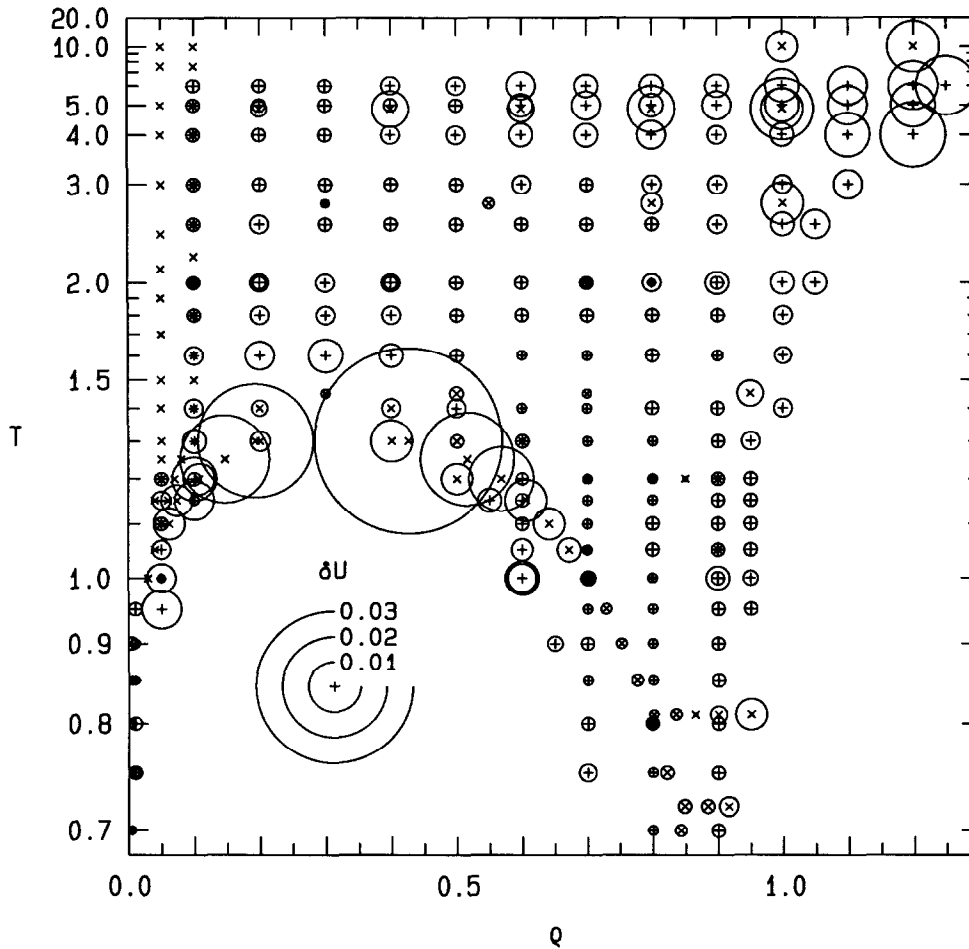
The errors in (Kolafa *et al.*, 1993) were calculated by the method based on summing the autocorrelation coefficients (Straatsma *et al.*, 1986); the errors of the new data were calculated by the above method combined with averaging in blocks of increasing lengths (Flyvbjerg and Petersen, 1989). We believe that such method makes use of almost all information contained in the measured (pseudo)time series and provides thus the best estimate of the error.

Fig. 1 The distribution of the simulation data on  $P$  in the  $\rho - T$  plane along with their statistical errors, reduced by the hard sphere fluid pressures given by the WCA theory. The parameters of the developed EOS were regressed from these data. +: Johnson *et al.* (1993);  $\times$ : Lotfi *et al.* (1992), our data, and the virial expansion. Circles in the left-lower corner give the scale of the errors



All state points used for the regression with the pseudoexperimental errors of  $P$  and  $U$  are shown in Figs. 1 and 2, respectively. Note that the errors of the pressure have been divided by the pressure of the reference HS fluid given by the WCA diameters (see *Appendix B*). This is because we need a quantity which has uniformly distributed errors. Neither pressure nor the compressibility factor are satisfactory: Errors at high densities are much larger than those at low densities. The relative error of pressure cannot be used either because pressure for metastable states close to the vapor-liquid coexistence line may be zero or even negative. The problem is that the pressure can be viewed as a

Fig. 2 The distribution of the simulation data on  $U$  in the  $\rho - T$  plane along with their statistical errors. For symbols see Fig. 1



difference of two comparably large contributions, a hard-sphere-like part which is positive and the mean-field attraction which is negative. A generalization of the 'relative' error is to reduce the error by the positive part which can be approximated by the WCA theory. We only recall that this trick has been used purely for the purpose of the figures to make them instructive and nice looking.

### Systematic errors

In pseudoexperiments we have to approximate infinite systems by small finite systems, usually cubic samples in the periodic boundary conditions. In addition, it is necessary to cut off, and often also to shift, the potential. All these approximations introduce systematic errors into the measured thermodynam-

ic quantities. (In this paper we do not consider other sources of systematic errors like inaccurate integration of the equations of motion, biased sampling in MC, *etc.*, because it is believed that the pseudoexperiments were carried out properly.)

Anisotropy imposed by periodic boundary conditions is, with the current accuracy, negligible for more than 500 atoms (Kolafa, 1992). This cannot be said about the effects caused by the influence of a finite sample on fluctuations of thermodynamic quantities. To estimate them let us consider different thermodynamic ensembles. The infinite system limit (the thermodynamic limit) should be the same for all ensembles. This does not say anything about the rate of convergence, that is, we do not know which ensemble with finite-size sample approximates better the infinite one. The differences between ensembles are caused by different fluctuations of quantities; *e.g.* in an isochoric ensemble the volume is constant while the pressure fluctuates, and vice versa for an isobaric ensemble. We can only conjecture that the best approximation is obtained by a grand canonical ensemble which allows exchange of particles and approximates thus in the best way a finite sample cut out from an infinite system. Then, an NPT ensemble might work better than an NVT one, at least for measuring EOS. The microcanonical ensemble is subject to most constraints that suppress fluctuations of density and local entropy and will be probably the worst one.

Using the NPT probability distribution and the assumption that the fluctuating quantity  $X$  has the Gaussian distribution, one can derive the first order approximation to the difference of the expectation values of  $X$  in NPT and NVT ensembles (Allen and Tildesley, 1987):

$$\langle X \rangle_{\text{NPT}} - \langle X \rangle_{\text{NVT}} = \frac{1}{2} \text{Var } V \frac{\partial^2 X}{\partial V^2} \quad (25)$$

where  $V = N/\rho$  is the total volume and  $\text{Var } V = -T/(\partial P/\partial V)_T$ . Similarly, for the grand canonical ensemble

$$\langle X \rangle_{\mu\text{VT}} - \langle X \rangle_{\text{NVT}} = \frac{1}{2} \text{Var } N \frac{\partial^2 X}{\partial N^2} \quad (26)$$

where  $\text{Var } N = -T\rho^{-2}/(\partial P/\partial V)_T$ .

Unfortunately, we have not been able to relate the microcanonical ensemble, neither the ‘scaled velocity microcanonical’ or ‘friction thermostat’ ensemble (which is used in molecular dynamics to keep the kinetic temperature constant), to other ensembles. We only can conjecture that the mechanism leading to finite-size effects is the same for these ensembles as for the above mentioned ones so that our consequences will hold *qualitatively* as well.

Similar considerations can be drawn on the influence of the cut-off (and possibly shifted) potential. If the cutoff equals one half of the box size and the potential has the leading term of  $r^{-6}$ , the cutoff correction in both cases is proportional to  $1/N$ . The common method assuming  $g(r) = 1$  outside the cut-off sphere does not account for the change in the particle-particle correlations, or in other words density fluctuations. The errors are much smaller, but they

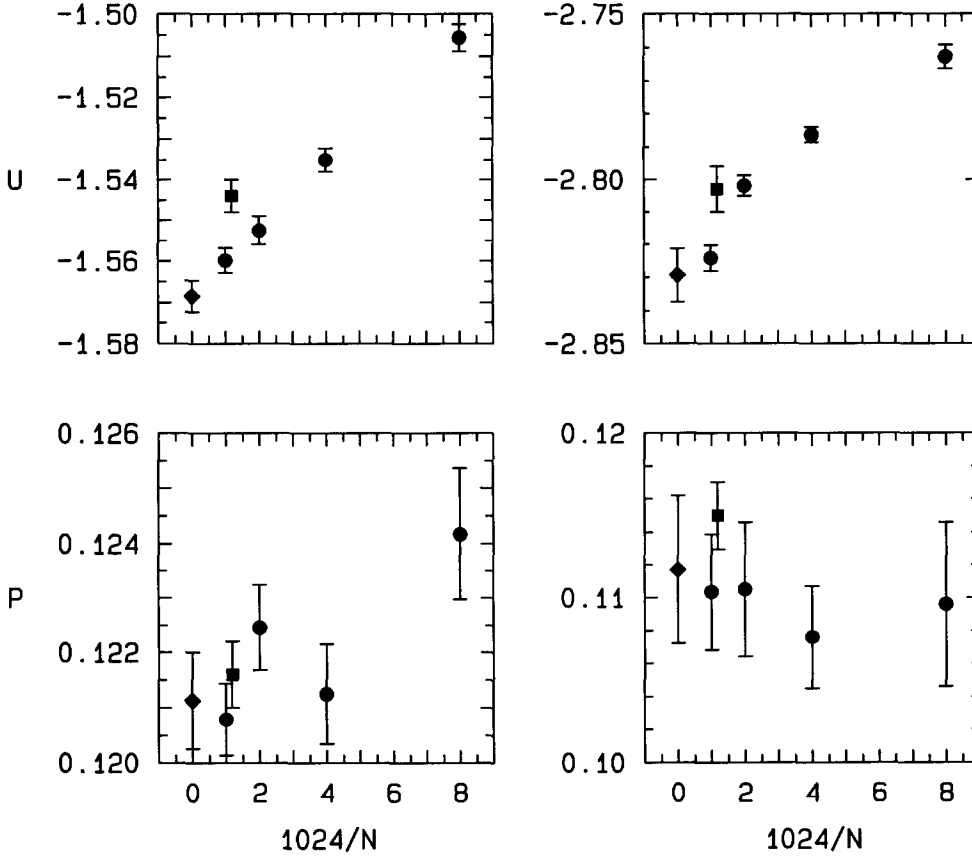
are still of the order of  $1/N$ . The mechanism is the same as the mechanism leading to the difference between ensembles, and thus we do not expect larger systematic errors than already estimated by the difference between ensembles.

We have compared the statistical errors of all  $P$  and  $U$  data (adjusted as described in the previous Section) with the systematic errors approximated by the differences (25) and (26) calculated using the JZG EOS. The largest systematic errors estimated by (26), several times larger than the statistical ones, occur in the critical region and for the metastable superheated liquid. We thus discarded several such points from the Johnson *et al.* (1993) set and also increased the errors of some other points. From the set of data by Kolafa *et al.* (1993) we removed all the data with small  $N$  and increased errors of some other ‘too accurate’ points; some data were only used in extrapolations as mentioned below. We also observed small systematic differences both between our and Johnson *et al.* data, and between our data obtained in different ensembles (NPT and NVE), and with and without the potential shift, which are however fully explainable by the finite size effects.

To replace some of the discarded points, we ran our own MC and MD simulations in the close-to-critical region with ascending numbers of particles up to  $N = 1024$  and uniformly scaled conditions (with the cutoff equal to one half of the box size). Then we extrapolated the obtained quantities using the assumption (which follows from (25) and (26)) that the systematic error decreases as  $1/N$ ; see Fig. 3 for examples and Table 1 for the summary of the results. Before using the linear regression (with weights, as usual, inversely proportional to the errors) to extrapolate to  $1/N \rightarrow 0$  we observed the quantities graphically to discard small- $N$  points with deviation from linearity; we were quite pessimistic and preferred to have less accurate results obtained from a few points only rather than to introduce another systematic errors. The error of the extrapolation was calculated from the errors of the points by the error-propagation law. Another independent possibility is to estimate the error from the scattering of the points themselves without taking into account their known errors; since the number of points is small (3 or 4), this is inaccurate, but still a good (and successful) test of the accuracy of our data.

Formula (25) gives larger values (exceeding in several cases the statistical errors) for pressure at higher temperatures and much larger values for the internal energy in the critical region; in other words, energy is measured inaccurately in an NPT ensemble close to the critical point. The NPT data of Lotfi *et al.* (1992) have, however, even larger statistical errors of  $U$  so that this does not cause any problem. Though both (25) and (26) for pressure give comparable or slightly higher values than the (adjusted) statistical errors of the Lotfi *et al.* data, we did not apply any correction because we trust the true NPT ensemble for the density/pressure EOS more than the NVT, NVE, or even ‘scaled velocity microcanonical’ ensembles, and also because the data were obtained with the maximum cutoff.

Fig. 3 Dependence of the internal energy  $U$  and pressure  $P$  on the number of particles  $N$  for  $T = 1.3$  and  $\rho = 0.2$  (left) and  $\rho = 0.4$  (right). Circles: MC data; square: Johnson *et al.* (MD,  $N=864$ ); diamond: extrapolation from  $N \in \{1024, 512, 256\}$



## RESULTS AND DISCUSSION

We will now use all the theoretical expressions summarized in Section *Theoretical prerequisites* and all the simulation data reviewed in the previous Section for the derivation of an accurate theoretically-based EOS. The basic relation is the expression for the Helmholtz free energy by means of the reference term in the form of the damped perturbed virial expansion, eqn. (15), and of a residual term  $\Delta A$  which we write in the form of a polynomial in  $T^{1/2}$  and  $\rho$ :

$$\Delta A = \sum_{ij} C_{ij} T^{i/2} \rho^j \quad (27)$$

The final explicit expression for the Helmholtz free energy thus is

$$A = A_{\text{HS}} + \exp(-\gamma \rho^2) \rho T \Delta B_{2,\text{hBH}} + \sum_{ij} C_{ij} T^{i/2} \rho^j \quad (28)$$

where  $A_{\text{HS}}$  is given by eqn. (5) with  $\eta = \pi\rho d_{\text{hBH}}^3/6$ , and the functional forms for  $d_{\text{hBH}}$  and  $\Delta B_{2,\text{hBH}}$  will be discussed later and summarized, along with the pressure and energetic equations, in Section *Summary and conclusions*.

Exponents  $i$  in (28) may be both positive and negative and  $j \geq 2$  because the reference part has already the correct low density expansion up to  $\rho$ . The choice of the fraction exponents results from preliminary calculations and physical considerations (*cf.* the next Subsection).

The proposed expression for  $A$ , and hence for  $P$  and  $U$ , thus contains a number of adjustable parameters (and one non-linear parameter  $\gamma$  in (15)) in addition to the theoretically defined ingredients: the hard sphere diameter (see eqn. (17)) and the second virial coefficient. While the latter quantities may be approximated by analytic expressions using the method explained in Section *Functional approximation*, the adjustable parameters will be evaluated by simultaneously fitting the data on  $P$ ,  $U$ , and, when available, also on  $\mu$ .

Since the proposed EOS is analytical at the critical point, *i.e.* it gives the classical density critical exponent of  $1/2$  instead of the supposed value of about  $1/3$  based on the analogy with the Ising ferromagnet or lattice gas, it cannot accurately describe the region of temperatures and densities close to the critical point. We have seen in the preceding Section that accurate simulation data for this region are not available anyway and we ourselves must thus resign to an accurate description of the close-to-critical region. For the same reason, we will not constrain the critical point as *e.g.* Johnson *et al.* (1993).

With respect to the theoretical basis of the starting equation (15), the range of thermodynamic conditions (outside the critical region) over which the EOS will perform is basically limited only by the availability of experimental data which range from  $T = 0.7$  to  $T = 6$  with two points extended to  $T = 10$ . To allow extrapolations, we took the temperature interval for approximating the exactly known functions defining the reference wider, ranging from  $T = 0.68$  (the triple point) to  $T = 20$  (15 times the critical temperature). We only remind in passing that the JZG equation, with which we will compare our results, is restricted only to the range  $T \leq 6$ ; outside this range it loses very fast its accuracy.

### *The hard sphere diameter and residual second virial coefficient*

The hard sphere diameters defined by both eqn. (17) and eqn. (18) have been approximated analytically by several authors. The best of these seem the recent parameterizations by Nezbeda (1993) but neither his results are accurate enough to satisfy our requirements. As regards the second virial coefficient, the common expansion in powers of  $T^{-1/4}$  requires many coefficients to obtain the accurate result at low temperatures. Moreover, the final result for  $\Delta B_2$  would be then given by the difference of two approximate terms. We therefore prefer to apply the minimax approximation directly to the residual virial coefficient.

Since the temperature range over which eqn. (29) will operate is quite wide,  $T \in \langle 0.68, 20 \rangle$ , we will use the polynomials in (both positive and negative)



TABLE 2

Coefficients of the parameterization of the hard sphere diameter and residual second virial coefficient given by the hybrid Barker-Henderson theory. See (29) for the functional form

$d_{\text{hBH}}$		$\Delta B_{2,\text{hBH}}$	
$i$	$C_i$	$i$	$C_i$
-2	0.011117524	-7	-0.58544978
-1	-0.076383859	-6	0.43102052
0	1.080142248	-5	0.87361369
1	0.000693129	-4	-4.13749995
ln	-0.063920968	-3	2.90616279
		-2	-7.02181962
		0	0.02459877
$\epsilon'_{\text{max}}$	$1.67 \times 10^{-4}$	$\epsilon'_{\text{max}}$	$1.72 \times 10^{-3}$
$\epsilon_{\text{max}}$	$9.05 \times 10^{-5}$	$\epsilon_{\text{max}}$	$4.81 \times 10^{-4}$

TABLE 3

Coefficients of the PVE/hBH equation of state, see eqns. (30)–(32)

$i$	$j$	$C_{ij}$	$i$	$j$	$C_{ij}$	$i$	$j$	$C_{ij}$
0	2	2.01546797	-1	5	93.92740328	-4	2	-13.37031968
0	3	-28.17881636	-1	6	-27.37737354	-4	3	65.38059570
0	4	28.28313847	-2	2	29.34470520	-4	4	-115.09233113
0	5	-10.42402873	-2	3	-112.35356937	-4	5	88.91973082
-1	2	-19.58371655	-2	4	170.64908980	-4	6	-25.62099890
-1	3	75.62340289	-2	5	-123.06669187			
-1	4	-120.70586598	-2	6	34.42288969	$\gamma$		1.92907278

powers of  $x = T^{1/2}$  to make the range effectively narrower. A general form of our analytic approximation of functions given by one-dimensional integrals is therefore

$$f(T) = \sum_i C_i T^{i/2} + C_{\ln} \ln T \quad (29)$$

As mentioned earlier, we calculate first the minimax approximation for the derivative  $f' = \partial f / \partial (1/T)$  and then we integrate it to obtain the final approximation for  $f$ ; the term  $\ln T$  is then a result of the integration of the term  $1/T$ .

A sufficiently accurate approximation of  $d_{\text{hBH}}(T)$  requires 5 constants while that for the corresponding  $\Delta B_{2,\text{hBH}}(T) = B_{2,LJ} - 2\pi d_{\text{hBH}}^3/3$ , requires 7 constants. The obtained constants along with the errors of the parameterization of both quantities are listed in Table 2.

TABLE 4

Comparison of different equations of state for the Lennard-Jones fluid.  $\gamma$  is the nonlinear parameter,  $D$  is the total standard deviation (22),  $D_P$ ,  $D_U$  and  $D_\mu$  are the partial deviations (24) for subsets of data for pressure, internal energy, and chemical potential, respectively, and  $\delta_{\max}$  is the maximum deviation (23)

EOS	$\gamma$	$D$	$D_P$	$D_U$	$D_\mu$	$\delta_{\max}$	$T_{\text{crit}}$	$P_{\text{crit}}$	$\rho_{\text{crit}}$
PVE/hHB <sup>a</sup>	1.929	1.440	1.316	1.594	1.028	8.25	1.3396	0.1405	0.3108
PVE/hHB <sup>b</sup>	1.911	1.427	1.303	1.579	1.025	8.24	1.3396	0.1406	0.3111
PVE/WCA	1.383	1.620	1.468	1.796	1.218	8.18	1.3436	0.1409	0.3070
MBWR	3	7.718	2.968	11.084	3.184	93.68	1.3506	0.1452	0.3220
MBWR <sup>c</sup>	3	4.228	1.353	6.123	1.525	22.23	1.3383	0.1414	0.3166
MBWR <sup>cd</sup>	4.52	4.197	1.372	6.076	1.427	22.17	1.3393	0.1421	0.3204
JZG <sup>e</sup>	3	6.118	2.468	7.981	—	26.77	1.313	0.1299	0.31
JZG <sup>cf</sup>	3	5.345	2.437	6.571	7.864	36.47	1.313	0.1299	0.31
JZG <sup>f</sup>	3	10.344	3.538	14.129	10.953	155.33	1.313	0.1299	0.31
NGST <sup>cg</sup>	3	8.340	6.082	9.152	11.553	43.98	1.35	0.1418	0.35

<sup>a</sup> EOS proposed in this paper, see Table 3 and eqns. (30)–(32)

<sup>b</sup> more accurately fitted reference

<sup>c</sup> points with  $T > 6$  have been excluded from the data set

<sup>d</sup> optimized non-linear parameter  $\gamma$ , see Table 5

<sup>e</sup> EOS and data set of Johnson *et al.* (1993)

<sup>f</sup> EOS of Johnson *et al.* (1993) with our data set

<sup>g</sup> EOS of Nicolas *et al.* (1979) with our data set

## Equations of state

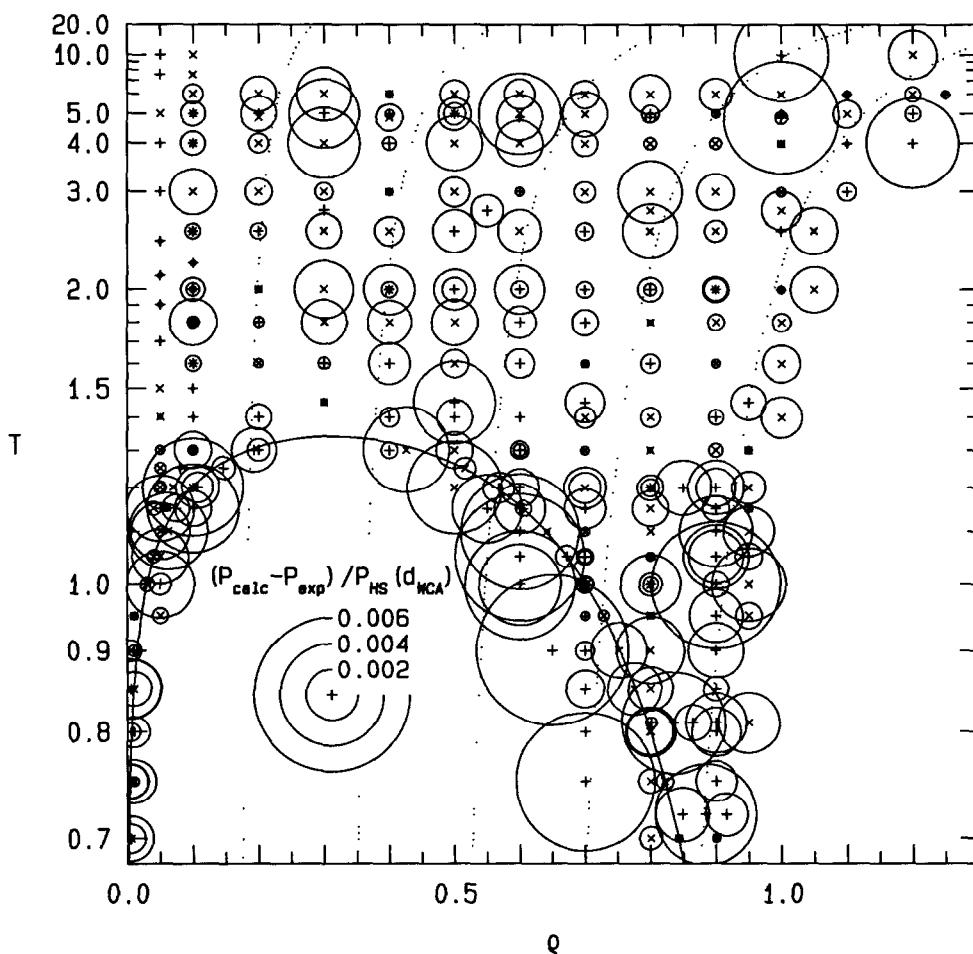
### Perturbed-virial-expansion-type equation

With the reference hard-sphere terms being now available in the closed analytic form, it remains to evaluate parameters  $C_{ij}$  of the residual term and the non-linear parameter  $\gamma$  appearing in eqn. (28).

We have tried to use expansion (27) with different number of adjustable parameters  $C_{ij}$  as well as with different exponents. A reasonable compromise between complexity and accuracy has been reached with 19 parameters  $C_{ij}$ .

Table 3 gives the parameters of the EOS which uses the hBH  $T$ -dependent diameters while Table 4 summarizes the standard deviations, maximum error and the calculated critical point. The deviations of this EOS from the simulation data for pressure and internal energy are shown in Figs. 4 and 5. These should be compared to the experimental errors, Figs. 1 and 2. For completeness we show in Figs. 6 and 7 also the relative deviations (the deviations divided by the experimental errors) of  $P$  and  $U$ ; we remind that the sum of the areas of the circles is proportional to  $D_P^2$  and  $D_U^2$  (see eqn. (24)) and that the radius of the largest circle equals the maximum relative error  $\delta_{\max}$ , eqn. (23).

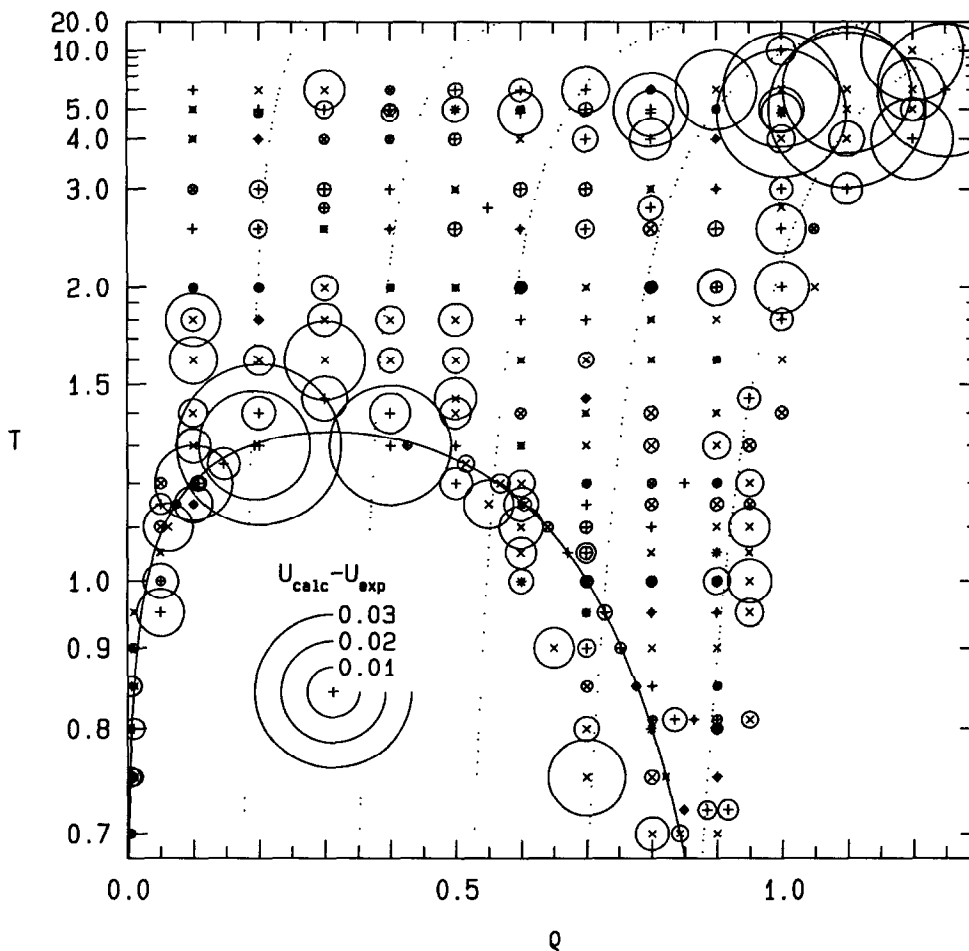
Fig. 4 Deviations of the PVE/hBH EOS for pressure from the simulation data, reduced by the hard sphere fluid pressures given by the WCA theory. Circles in the left-lower corner give the scale of the errors, positive values are marked by +, negative ones by  $\times$ . The dotted lines are the HS isochores for the packing fraction  $\eta = \pi \rho d_{\text{hBH}}^3/6$  going from 0.1 to 0.5 by 0.1 and the solid line is the calculated vapor-liquid coexistence curve



The standard deviation  $D = 1.4398$  is close to unity which suggests that we are quite close to the ideal correlation, although we must be aware of the fact that we, in average, have increased the statistical errors so that the value of  $D$  for an ideal correlation would be lower than 1.

As a test of our approach we repeated the calculations with  $d_{\text{hBH}}$  and  $\Delta B_{2,\text{hBH}}$  replaced by more accurate functions (with 6 and 8 parameters, respectively). The difference was very small, see Table 4, and we may thus conclude that the errors in  $d_{\text{hBH}}$  and  $\Delta B_{2,\text{hBH}}$  do not affect the quality of the EOS. We also repeated these calculations with the reference HS given by the WCA temperature and

Fig. 5 Deviations of the internal energy given by the PVE/hBH EOS from the simulation data. See Fig. 4 for details

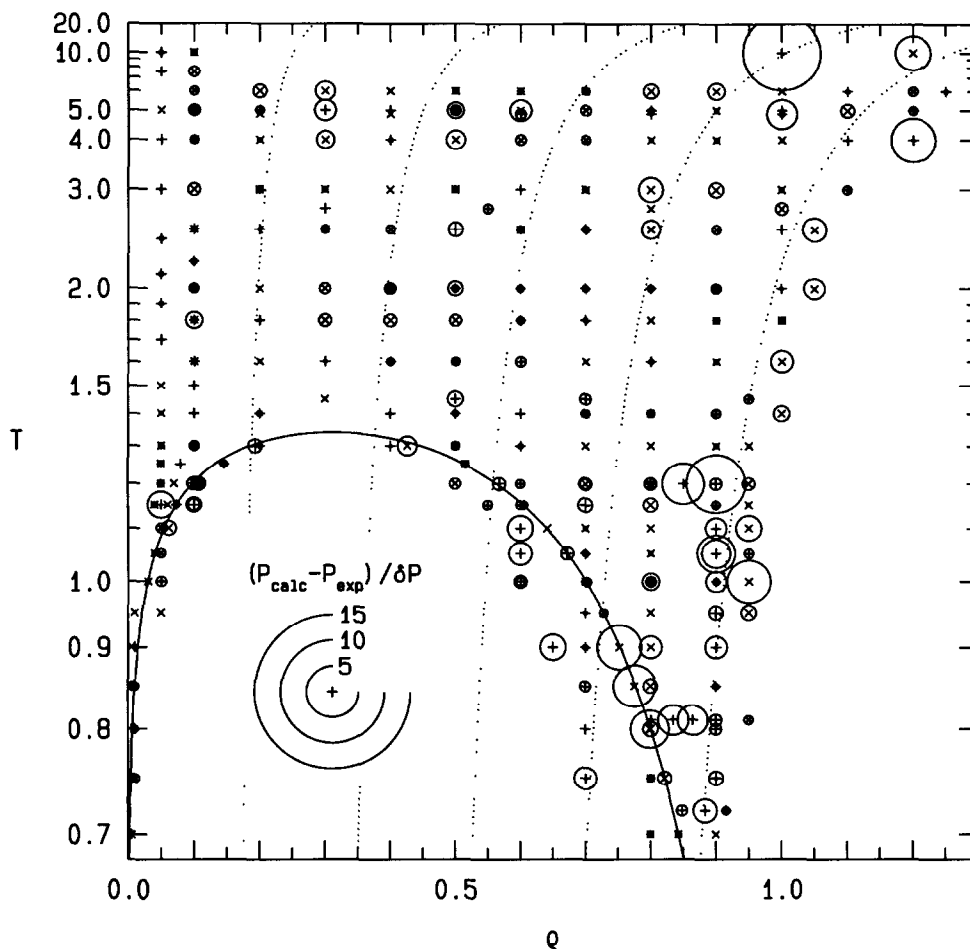


density dependent diameter. Surprisingly, it appeared that this approach produced worse results.

#### Modified Benedict-Webb-Rubin equation

The JZG equation was originally derived by fitting a MBWR-type equation to a slightly different set of data and with the constrained critical temperature and density. Although we also compare our new equation directly with the JZG equation in Table 4, for a fair comparison between the MBWR and PVE-type equations we re-fitted the MBWR equation using our data set. We took the 5 parameters describing the second virial coefficient from Johnson *et al.* (1993) and regressed the remaining 28 parameters; similarly to Johnson *et al.*

Fig. 6 The same as figure 4 with the deviation of pressure reduced by the experimental errors

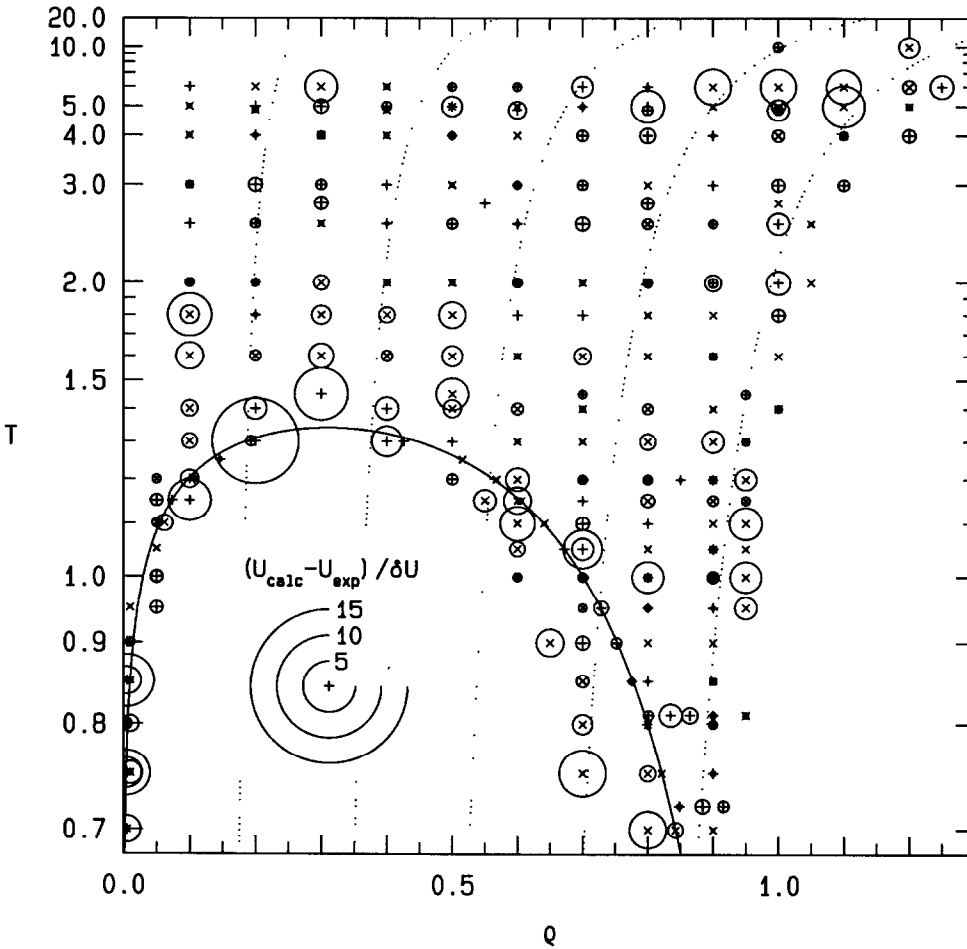


we observed numerical problems with simultaneous regressing all 27 linear and one nonlinear parameter and had to find the optimum value of the nonlinear parameter by a manual search. It appeared that the worst problems were at high temperatures and densities and thus we repeated the calculations excluding the range  $T > 6$ . Though the standard deviation decreased twice, it was still three times larger than that for the PVE equations. The coefficients of this correlation are given in Table 5 and the deviations from the simulation data in Figs. 8 and 9.

#### *Comparison of equations of state*

Examination of Table 4 demonstrates accuracy of the PVE/hBH equation of state throughout the entire  $\rho - T$  plane and its clear superiority over the

Fig. 7 The same as figure 5 with the deviation of the internal energy reduced by the experimental errors



remaining equations considered. It is also seen from the values of the partial standard deviations that the more significant improvement was reached for the internal energy; the internal energy is described by PVE/hBH only slightly worse than pressure.

It is seen from Figs. 6 and 7 that there are two regions where the fit of the PVE/hBH equation is worse than a few standard deviations: The region close to the critical point where our classical EOS cannot describe the non-classical behavior in principle, and the high-temperature and high-density region.

As regards the analogous equation based on both density and temperature dependent WCA diameter of the reference HS fluid (see *Appendix B*), it is seen from Table 4 that, surprisingly, the resulting EOS is slightly worse than that based on the hBH diameters. We thus may conclude that the 'better' density

TABLE 5

Coefficients of the MBWR equation of state, regressed from data with  $T \leq 6$ . See Johnson *et al.* (1993) for notation

$i$	$x_i$	$i$	$x_i$	$i$	$x_i$
1	0.86230851	12	-41.33848427	23	24.87520514
2	2.97621877	13	15.14482295	24	-6246.96241113
3	-8.40223012	14	88.90243729	25	-235.12327760
4	0.10541366	15	-2425.74868591	26	-7241.61133138
5	-0.85645838	16	-148.52651854	27	-111.27706706
6	1.39945300	17	68.73779789	28	-2800.52326352
7	-0.20682219	18	2698.26346845	29	1109.71518240
8	2.66555449	19	-1216.87158315	30	1455.47321956
9	1205.90355811	20	-1199.67930914	31	-2577.25311109
10	0.24414200	21	-7.28265251	32	476.67051504
11	6.17927577	22	-4942.58001124	$\gamma$	4.52000000

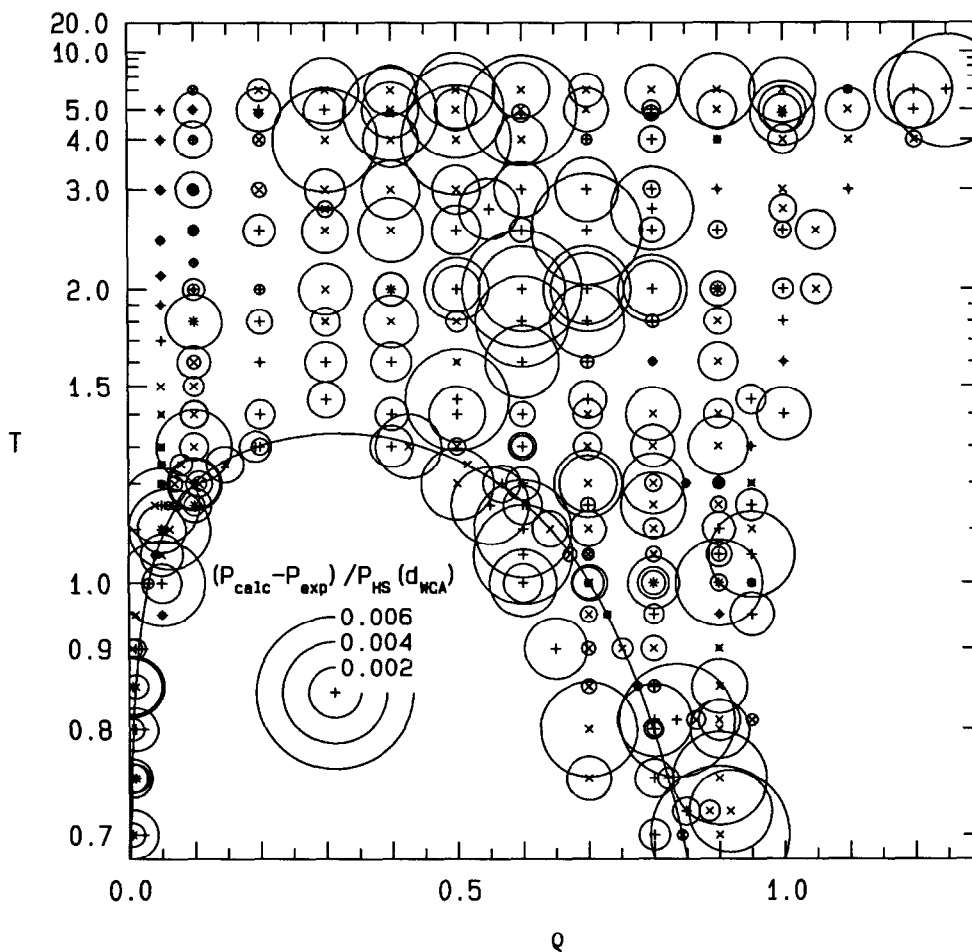
dependent diameter need not necessarily lead to a better EOS, mainly because the dependence on density is already captured, to a great extent, by residuum (27). In addition, the EOS based on  $d_{\text{WCA}}$  is *considerably* more complicated than the EOS based on  $d_{\text{hBH}}$ .

It is seen from Figs. 8 and 9 that the only region in which the MBWR EOS for pressure may seem to work slightly better than PVE/hBH is the range of cold dense liquid. The worst metastable points have, however, large experimental errors (in fact, we have enlarged these errors, as described in Section *Simulation data*). Examination of the relative errors  $(P_{\text{calc}} - P_{\text{exp}})/\delta P$  shows that all EOS are equally good in this region. The problems are (again) connected with the quality of the simulation data: Data from different sources differ more than it could be expected from the experimental errors.

Rapid deterioration of the MBWR equation for internal energy at higher temperatures and densities is caused by an insufficient number of  $T$ -dependent terms. This is a consequence of the fact that this equation concentrates on pressure rather than on both pressure and energy simultaneously. This also includes the inaccurate derivative of the second virial coefficient. Only 5 constants reserved for the low density limit are not enough to have a sufficiently accurate both the derivative and the second virial coefficient itself, see Fig. 10.

The last property which we have included into the calculations to check the performance of the considered EOS is the vapor-liquid coexistence. The vapor-liquid equilibrium pressures calculated from different equations are plotted in Fig. 11 in the form of relative deviations from the recent parameterization by Lotfi *et al.* (1992); the original data on which the parameterization is based (simulation data with 1372 atoms on both the gas and liquid phases) are also shown. The density-temperature coexistence curves are shown in Fig. 12 along with the Lotfi *et al.* parameterization and data. It is seen that the JZG equation

Fig. 8 Deviations of the MBWR EOS for pressure from the simulation data, reduced by the hard sphere fluid pressures given by the WCA theory. See Fig. 4 for details. Note that points with  $T > 6$  have been excluded

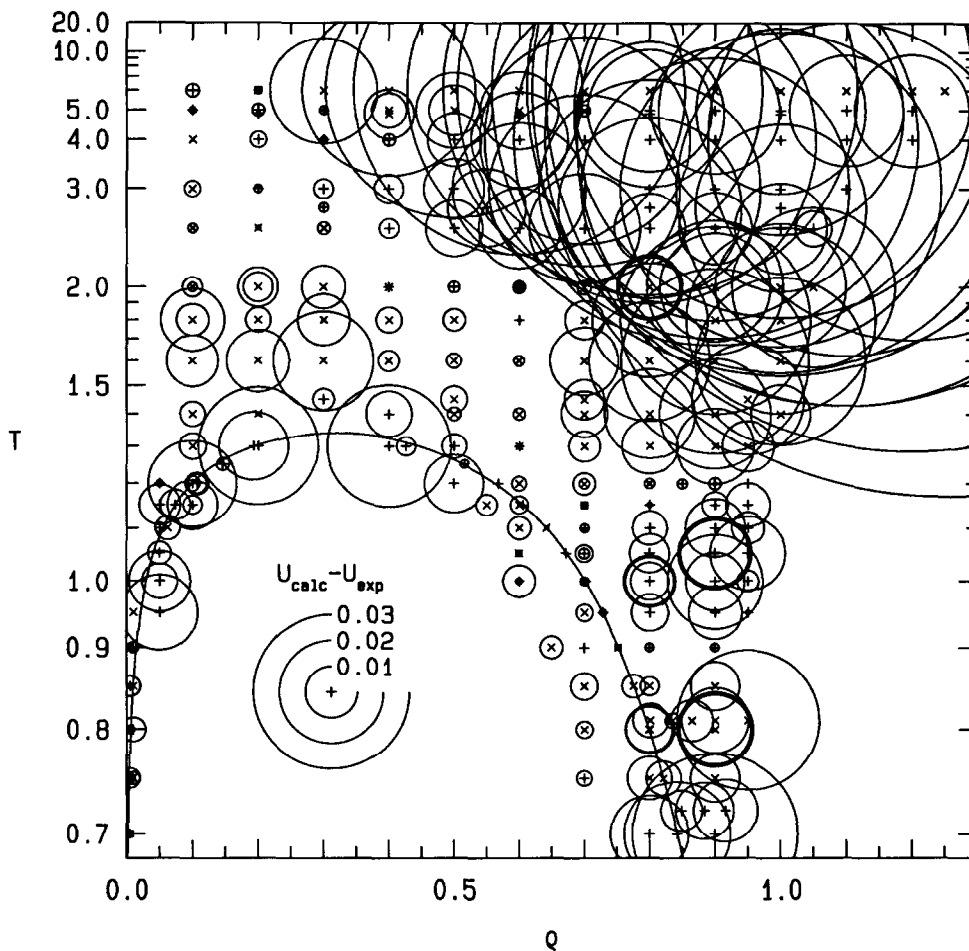


differs from the simulation-based data slightly more than their error bars. Our equations, both MBWR and PVE/hBH, fit the data better (we however used better simulation data in the critical region, including the data by Lotfi *et al.* themselves). On the other hand, we have not constrained the critical point so that its value and the vapor-liquid coexistence curve in its vicinity is worse. Since—as we have already mentioned—the classical EOS cannot describe the critical region and no good data in this region are available, we prefer to resign on the location of the critical point and have better EOS outside the close vicinity of the critical point.

For comparison we have also included into the figures the orthobaric pressure given by the older version of the MBWR equation, EOS due to Nicolas *et*



Fig. 9 Deviations of the internal energy given by the MBWR EOS from the simulation data. See Fig. 8 for details



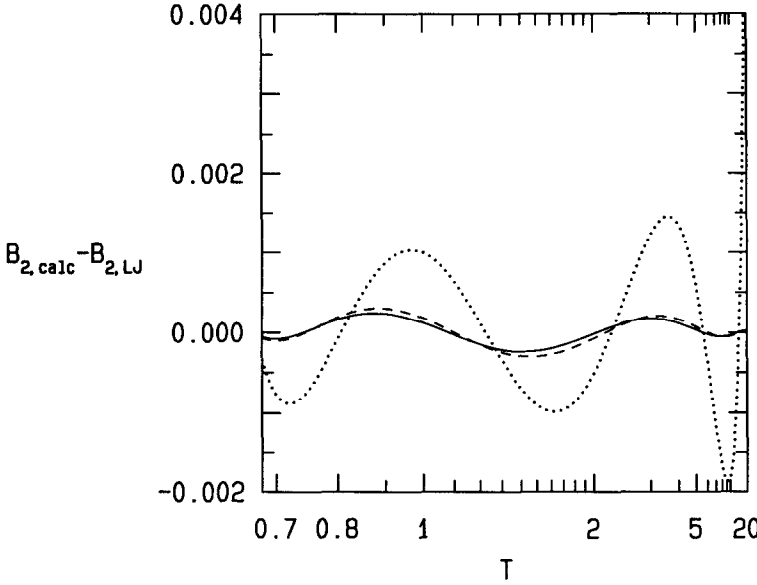
*al.* (1979). As it is seen, this equation gives the pressure which is, for all temperatures but the lowest, outside the experimental data.

## SUMMARY AND CONCLUSIONS

This paper accomplishes the series of papers devoted to applications of results of modern molecular theories of liquids and its main goal has been to clearly demonstrate that there is no reason why the theoretical results should be ignored by engineers and that they may form a firm and sound basis for developing accurate analytic expressions for properties of real fluids.

We have focused on developing closed analytic expressions for the thermodynamic properties of the Lennard-Jones fluid whose accuracy would be compara-

Fig. 10 Errors of the second virial coefficient given by the low density limit of different EOS. Dotted line: MBWR, Johnson *et al.* (1993); solid line: PVE/hBH; dashed line: PVE/WCA



ble with or better than that of the best available to date. The main ingredients of the method which yield the best results have been (i) the perturbed virial expansion and (ii) the hybrid Barker-Henderson recipe for the temperature dependence of the size of the reference hard spheres. The empirical correction term has been written in the form of a simple polynomial in density and temperature.

For completeness, we repeat here the final expression for the Helmholtz free energy (28) and give also the corresponding pressure and energetic equations of state

$$A = A_{\text{HS}} + \exp(-\gamma\rho^2) \rho T \Delta B_{2,\text{hBH}} + \sum_{ij} C_{ij} T^{i/2} \rho^j \quad (30)$$

$$z \equiv \frac{P}{\rho T} = z_{\text{HS}} + \rho(1 - 2\gamma\rho^2) \exp(-\gamma\rho^2) \Delta B_{2,\text{hBH}} + \sum_{ij} j C_{ij} T^{i/2-1} \rho^j \quad (31)$$

$$U = \frac{3(z_{\text{HS}} - 1)}{d_{\text{hBH}}} \frac{\partial d_{\text{hBH}}}{\partial(1/T)} + \rho \exp(-\gamma\rho^2) \frac{\partial \Delta B_{2,\text{hBH}}}{\partial(1/T)} - \sum_{ij} \left(\frac{i}{2} - 1\right) C_{ij} T^{i/2} \rho^j \quad (32)$$

where  $A_{\text{HS}}$  and  $z_{\text{HS}}$  are given by eqns. (5) and (4), respectively, with  $\eta = \pi\rho d_{\text{hBH}}^3/6$ , functions  $d_{\text{hBH}}$  and  $\Delta B_{2,\text{hBH}}$  are approximated by formula (29) with coefficients given in Table 2, their derivatives over  $1/T$  are

$$\frac{\partial f(T)}{\partial(1/T)} = -T \left( \sum_i \frac{i}{2} C_i T^{i/2} + C_{\ln} \right) \quad (33)$$

Fig. 11 Vapor pressures calculated from different EOS and expressed as relative differences from the parameterization by Lotfi *et al.* (1992); circles with error bars are their original data. Solid line: PVE/hBH; dotted line: MBWR,  $T \leq 6$ ; dash-dotted line: JZG; dashed line: Nicolas *et al.* (1979). Squares are the calculated critical points

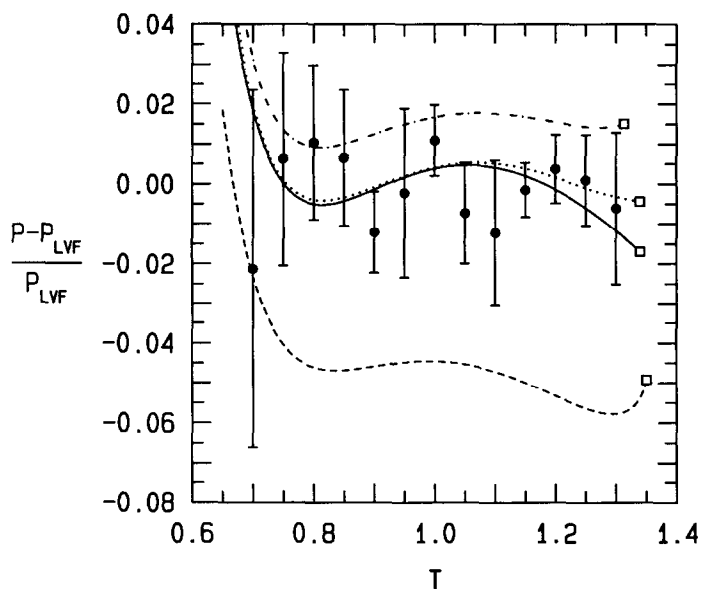
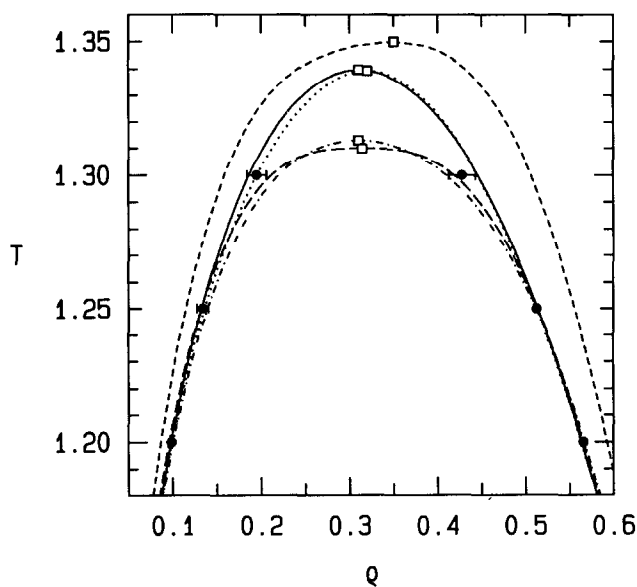


Fig. 12  $\rho - T$  coexistence curve in the vicinity of the critical point calculated from different EOS. The long-dash line is the parameterization by Lotfi *et al.* (1992), for other symbols see Fig. 11



and finally constants  $C_{ij}$  are given in Table 3.

The range of temperatures over which the above equations yield accurate results stretches from the triple point,  $T \approx 0.68$ , up to  $T \approx 10$ . The equations are thermodynamically self-consistent which means that their results are of the same accuracy for different thermodynamic quantities. For the physical reasons the experimental data on the critical point have not been included into the set of data used for the evaluation of the parameters  $C_{ij}$ . The critical parameters given by eqn. (31) are

$$T_{\text{crit}} = 1.3396, \quad P_{\text{crit}} = 0.1405, \quad \rho_{\text{crit}} = 0.3108 \quad (34)$$

and yield the critical compressibility factor  $z_{\text{crit}} = 0.3375$  in agreement with mean field theories.

It has been shown that, despite the fact that eqn. (31) has less parameters than the MBWR-type equation of Johnson *et al.* and covers a larger range of temperatures, it performs better, especially for the internal energy. Because of its underlying molecular nature, the proposed EOS is also much better than the JZG equation when extrapolated outside their respective ranges of temperature.

There has been a deeply rooted prejudice, among both theorists and engineers, that a perturbed hard sphere EOS, despite its sound theoretical basis, cannot produce results of high accuracy. This may be true if *only* the hard sphere term is combined with an empirical correction. Within the employed concept of a molecular-thermodynamic reference, a reference system is made up of a hard sphere term *and* another theoretical term. This choice guarantees that the most difficult and complicated part of the behavior of thermodynamic functions is accounted for correctly by such a reference and that only a simple empirical correction is required to reach the required accuracy. The above equations are based on the reference defined by a perturbed virial expansion, *i.e.* on the simplest and most general choice considered. This choice has not been made arbitrarily but has resulted from calculations in which several methods have been considered. This finding along with the fact that the best results are based also on only temperature-dependent reference hard sphere diameters has far reaching consequences: The method leading to the above equations for the LJ fluid can be readily extended to other potentials or types of liquids.

Our EOS is classical, *i.e.* it cannot describe accurately the region close to the critical point. An accurate EOS for the neighborhood of the critical point must take into account not only the correct critical exponents, but it also has to correlate accurate pseudoexperimental data, *i.e.* data obtained by a careful extrapolation to the thermodynamic limit. To produce such data is a challenging task for the best laboratories because one has to use large systems to overcome the large scale density fluctuations, and long runs to beat the critical slowing-down. There seems no other way to a *reliable* description of the critical region, including the location of the critical point itself.

## ACKNOWLEDGEMENT

We would like to thank Professor J. Fischer, University of Bochum, for his valuable comments concerning the presentation of the paper. This work was supported by grant 203/93/2284 of the Grant Agency of the Czech Republic and by grant 472401 of the Grant Agency of the Academy of Sciences.

## LIST OF SYMBOLS

$A$	Helmholtz free energy per molecule (without the ideal gas part)
$B_2$	second virial coefficient
$C_i, C_{ij}$	numerical constants and adjustable parameters
$D$	standard deviation of the regression, eqn. (22)
$D_S$	partial standard deviation for a subset of data $S$ , eqn. (24)
$d$	diameter of the reference hard spheres
$N$	number of atoms in the simulation box
$P$	pressure
$T$	temperature
$U$	configurational internal energy per molecule
$z$	compressibility factor
$\gamma$	nonlinear adjustable parameter
$\Delta B_2$	residual second virial coefficient, eqn. (16)
$\delta X$	statistical or experimental error of quantity $X$
$\delta_{\max}$	maximum relative deviation, eqn. (23)
$\epsilon_{\max}$	maximum error of the functional approximation
$\epsilon'_{\max}$	maximum error of the derivative of the functional approximation over $1/T$
$\eta$	packing fraction of the HS fluid, eqn. (3)
$\mu$	chemical potential per molecule (without the ideal gas part)
$\rho$	number density
crit	critical point
EOS	equation of state
hBH	hybrid Barker-Henderson
HS	hard sphere (fluid)
HTA	high temperature approximation
JZG	Johnson, Zollweg and Gubbins (1993) EOS
LJ	Lennard-Jones (fluid)
MD	molecular dynamics
MC	Monte Carlo simulation
MBWR	modified Benedict-Webb-Rubin EOS
MTR	molecular-thermodynamic reference
NGST	Nicolas, Gubbins, Streett and Tildesley (1979) EOS
ref	reference

res        residual (excess over the reference system)  
WCA       Weeks-Chandler-Andersen

## REFERENCES

- Aim, K. and Nezbeda, I., 1989. Thermodynamic properties of the Lennard-Jones fluid. I. *Fluid Phase Equilibria*, 48: 11–22.
- Allen, M.P. and Tildesley, D.J., 1987. *Computer simulations of liquids*. Clarendon Press, Oxford.
- Barker, J.A., Leonard, P.J. and Pompe, A., 1966. Fifth Virial Coefficients. *J. Chem. Phys.*, 44: 4206–4211.
- Boublík, T. and Nezbeda, I., 1986. P-V-T behaviour of hard body fluids. Theory and experiment. *Colln. Czech. Chem. Commun.* 51: 2301–2432.
- Boublík, T., Nezbeda, I., and Hlavatý, K., 1980. *Statistical Thermodynamic of Simple Liquids and Their Mixtures*. Elsevier, Amsterdam.
- Flyvbjerg, H. and Petersen, H.G., 1989. Error estimates on averages of correlated data. *J. Chem. Phys.*, 91: 461–462.
- Johnson, J.K., Zollweg, J.A. and Gubbins, K.E., 1993. The Lennard-Jones Equation of State Revisited. *Mol. Phys.*, 78: 591–618.
- Kolafa, J., 1992. Finite size effects for liquid in cyclic boundary conditions. *Mol. Phys.*, 75: 577–586.
- Kolafa, J., Vörtler, H.L., Aim, K. and Nezbeda, I., 1993. The Lennard-Jones fluid revisited: Computer simulation results. *Molec. Simul.*, 11: 305–319.
- Labík and Malijevský, 1989. Bridge function for hard spheres in high density and overlap region. *Mol. Phys.*, 67: 431–438.
- Lotfi, A., Vrabec, J. and Fischer, J., 1992. Vapour liquid equilibria of the Lennard-Jones fluid from the NpT plus test particle method. *Molec. Simul.*, 76: 1319–1333.
- Maitland, G. C., Rigby, M., Wakeham, W. A. and Smith, E. B., 1987. *Intermolecular Forces*. Clarendon Press, Oxford.
- Malijevský and Labík, 1987. The bridge function for hard spheres. *Mol. Phys.*, 60: 663–669.
- Nezbeda, I., 1993. Molecular-thermodynamic reference equations of state. *Fluid Phase Equilibria*, 87: 237–253.
- Nezbeda, I. and Aim, K., 1984. Perturbed hard-sphere equations of state of real fluids. II. Effective hard sphere diameters and residual properties. *Fluid Phase Equilibria*, 17: 1–18.
- Nezbeda, I. and Aim, K., 1987. Perturbed hard-sphere equations of state of real fluids. III. *Fluid Phase Equilibria*, 34: 171–188.
- Nezbeda, I. and Aim, K., 1989. On the way from theoretical calculations to practical equations of state. *Fluid Phase Equilibria*, 52: 39–46.
- Nezbeda, I. and Pavlíček, J., 1994. Application of primitive models of associating fluids to real systems. I. Equation of state of water. *Fluid Phase Equilibria*, submitted.
- Nicolas J.J., Gubbins K.E., Streett W.W., Tildesley D.J., 1979. Equation of state for the Lennard-Jones fluid. *Mol. Phys.*, 37: 1429–1454.
- Ralston, A., 1965. *A first course in numerical analysis*. McGraw-Hill, New York.
- Smith, W. R., 1973. Perturbation theory in the classical statistical mechanics of fluids, in *Statistical Mechanics*, Vol. 1, Specialist Periodical Report. Chemical Society, London.
- Straatsma, T.P., Berendsen, H.J.C. and Stam, A.J., 1986. Estimation of statistical errors in molecular simulation calculations. *Mol. Phys.*, 57: 89–95.
- Weeks, J.D., Chandler D. and Andersen H.C.: 1971. The role of repulsive forces in determining the equilibrium structure of simple liquids. *J. Chem. Phys.*, 54: 5237.

## APPENDIX A: SIMULATION DETAILS

In the simulation close to the critical region, the potential was cut-and-shifted with the potential cutoff equal one half of the box; the potential was smoothed close to the cutoff value. The numbers of one-step configurations ranged from about 4 million at  $N = 1024$  to 1–2 million at lower  $N$ ; in the MD points the MD times were 200–300 reduced time units.

In MC at the critical region the displacement was one half of the box; it is worth noting that for large systems with large compressibility and then large density fluctuations it is more efficient to have a low acceptance ratio and maximum displacement rather than the usual short displacement with acceptance ratio of 0.3. For instance, for  $T = 1.2$ ,  $\rho = 0.5$  and  $N = 1024$ , the acceptance ratio is as low as 3% if the maximum displacement is used, but the errors in the internal energy are less than half of the errors in the usual arrangement with the acceptance ratio of 0.3; the pressure is not so sensitive. The detailed explanation of this phenomenon was given by Kolafa (1992).

The MD algorithm used the Nosé canonical thermostat and the four-value Gear predictor-corrector integrator. Some points at higher temperatures and densities were obtained by MD with a cut-and-smoothed (not shifted) potential.

## APPENDIX B: THE PVE/WCA EQUATION

The WCA diameter of the reference HS,  $d_{\text{WCA}}$ , is given implicitly by equation (18) which requires the knowledge of the background correlation function  $y_{\text{HS}}(r; d)$ . The most accurate result for  $y_{\text{HS}}$  we get by solving the Ornstein-Zernike (OZ) integral equation which relates the total correlation function,  $h = g - 1$ , and the direct correlation function,  $c$ , via

$$\gamma(r_{12}) = \rho \int c(r_{13})[\gamma(r_{23}) + c(r_{23})] d\mathbf{r}_3 \quad (\text{B1})$$

where  $\gamma = h - c$  and  $r_{ij} = |\mathbf{r}_i - \mathbf{r}_j|$ . To solve this equation one must supply an additional closure relation. In its most frequently used form this relation expresses  $c(r)$  in terms of the bridge function  $B(r)$  (Boublík et al., 1980):

$$c(r) = \exp[-u(r)/T - B(r) + \gamma(r)] - \gamma(r) - 1 \quad (\text{B2})$$

The bridge function is given, in general, by an infinite sum of elementary diagrams. For the hard sphere fluid a closed analytic approximation,  $B_{\text{ML}}$ , is available, obtained by fitting a suitable functional form to all known structural and thermodynamic computer simulation data over the entire fluid range up to the density of freezing. For its explicit form we refer the reader to the original papers (Maličevský and Labík, 1987; Labík and Maličevský, 1989). Equation (1) along with  $B_{\text{ML}}$  and (2) constitutes the B-OZ theory, an ‘exact’ theory for the hard-sphere fluid. A brief account of our numerical method to solve it is given in *Appendix C*.

TABLE 6

Coefficients of the parameterization of the low density limit of the hard sphere diameter and of the residual second virial coefficient given by the WCA theory. See (29) for the functional form

$d_{\text{WCA},0}$		$\Delta B_{2,\text{WCA}}$	
$i$	$C_i$	$i$	$C_i$
–2	0.010860840	–7	–0.49028948
–1	–0.073873599	–6	0.03554298
0	1.079811879	–5	1.47927894
1	0.000421560	–4	–4.51620903
ln	–0.061913939	–3	2.92985909
		–2	–6.95561537
		0	–0.00260179
$\epsilon'_{\text{max}}$	$1.75 \times 10^{-4}$	$\epsilon'_{\text{max}}$	$2.12 \times 10^{-3}$
$\epsilon_{\text{max}}$	$9.50 \times 10^{-5}$	$\epsilon_{\text{max}}$	$6.06 \times 10^{-4}$

The WCA diameter (18) is a function of two variables. Following the strategy used for the hBH diameter, we first separate the density-independent part  $d_{\text{WCA},0}$ ,

$$d_{\text{WCA}}(T, \rho) = d_{\text{WCA},0}(T) + d_{\text{WCA}}^*(T, \rho) \quad (\text{B3})$$

where

$$d_{\text{WCA},0}^3(T)/3 = \int_0^{R_m} \{1 - \exp[-\beta u_0(r)]\} r^2 dr \quad (\text{B4})$$

which may be approximated, along with the associated residual  $\Delta B_{2,\text{WCA}} = B_2 - 2\pi d_{\text{WCA},0}^3/3$ , in the same way as the  $\Delta B_{2,\text{hBH}}$ . The results of these parameterizations are given in Table 6.

The remaining residual part  $d_{\text{WCA}}^*(T, \rho)$  is small. The physical considerations suggest to express it using the packing fraction of the reference HS, which is approximated at a zeroth level by

$$\eta_0 = \frac{\pi}{6} \rho d_{\text{WCA},0}^3 \quad (\text{B5})$$

Further, considerations on derivatives of  $y_{\text{HS}}(r; d_{\text{WCA}})$  at contact suggest using terms containing  $\eta_0/(1 - \eta_0)$ . Our proposal for a suitable functional form is therefore

$$d_{\text{WCA}}^*(T, \rho) = \frac{\eta_0}{1 - \eta_0} \sum_{ij} C_{ij} T^{i/2} \rho^j \quad (\text{B6})$$

where  $j \geq 0$ .

Unlike the  $\rho \rightarrow 0$  limits considered above and which are defined by integrals and are thus available with an arbitrary precision, the residual term  $d_{\text{WCA}}^*(T, \rho)$  is subject to experimental errors because it is based on the parameterization of



TABLE 7

Coefficients of the parameterization of the residual term  $d_{\text{WCA}}^*$ , equation (B6)

$i$	$j$	$C_{ij}$	$i$	$j$	$C_{ij}$	$i$	$j$	$C_{ij}$
0	0	-0.013080068	0	1	-0.000907374	-2	2	0.013361019
-1	0	0.015907460	-1	1	-0.001603276	0	3	0.002575066
-2	0	-0.004823366	-2	1	-0.005481792	-2	3	-0.007824455
1	0	-0.000704171	0	2	-0.005172759			

the hard-sphere bridge function  $B_{\text{ML}}$ . In addition, we also need an expression for packing fractions significantly higher than  $\eta > 0.5$ , *i.e.* in the range where the HS fluid is metastable. Consequently, the bridge function must be extrapolated and the resulting HS diameters must be thus assessed with caution.

We use the least-square minimization method to find the approximation. To do this, we have generated 480 points covering the range of temperatures  $T \in \langle 0.68, 20 \rangle$  and densities in which at least metastable liquid may exist, including points in the two-phase region. The simulation state points (see Figs. 1 and 2) are subset of this set. For each point we calculated  $d_{\text{WCA}}$ , but not  $\partial d_{\text{WCA}} / \partial(1/T)$ . Since we also wish to have this derivative fitted accurately, and the derivative is usually least accurate on the border of the region of variables, we used higher weights (lower errors  $\delta X_i$  in eqn. (21)) for points close to the border of the interval  $T \in \langle 0.68, 20 \rangle$ . An accuracy better than  $1 \times 10^{-4}$  is reached with 11 parameters, see Table 7 and Fig. 13.

The diameter  $d_{\text{WCA}}$  given by (3) is more complicated than the recent explicit parameterization due to Nezbeda (1993) but is much more accurate (by one order for  $T \leq 6$  and  $\rho \leq 1.25$  and even more if we go to higher  $T$  and  $\rho$ ). In addition, it is based on the accurate limit  $d_{\text{WCA},0}$  which, in turn, makes it possible to introduce the accurate second virial coefficient into the final EOS.

## APPENDIX C: NUMERICAL SOLUTION OF THE OZ EQUATION

The OZ equation with closure (2) was solved by direct iterations with the damping (mixing) parameter adjusted in the course of the calculations (Kolafa, 1992). The convolutions were calculated by the fast Fourier transform; a correction was added to suppress oscillations arising when two jump functions are convoluted by the discrete Fourier transform. With this correction, the error is proportional to square of the grid (integration step in  $r$ ). Consequently, we used grids of  $1/64$  and  $1/128$  and Richardson extrapolation (Ralston, 1965, eqn. (4.12-20)). The integration range was 12 for the highest densities and lower for easy points at low densities. Control calculations give that the results are correct to 6 decimal digits which is more than sufficient.

Fig. 13 Errors of the fit of the WCA hard-sphere diameter, equation (3). Circles in the right-lower corner give the scale of the errors, positive values are marked by +, negative ones by  $\times$ . The dotted lines are the HS isochores for the packing fraction  $\eta = \pi \rho d_{\text{WCA}}^3/6$  going from 0.1 to 0.5 by 0.1

